

1 The generation of HepG2 transmitochondrial cybrids to reveal the role of mitochondrial genotype in  
2 idiosyncratic drug-induced liver injury: a translational *in vitro* study

3  
4

5 Amy L. Ball<sup>1</sup>, Carol E. Jolly<sup>1</sup>, Jonathan J. Lyon<sup>2</sup>, Ana Alfirevic<sup>3</sup>, Amy E. Chadwick<sup>1\*</sup>

6 <sup>1</sup> MRC Centre for Drug Safety Science, Department Pharmacology and Therapeutics, University of  
7 Liverpool, Liverpool, UK

8 <sup>2</sup> GSK GlaxoSmithKline, Safety Assessment, Ware, UK

9 <sup>3</sup> The Wolfson Centre for Personalised Medicine, Department Pharmacology and Therapeutics,  
10 University of Liverpool, Liverpool, UK

11 \*Corresponding Author. E-mail: [aemercer@liverpool.ac.uk](mailto:aemercer@liverpool.ac.uk), Tel: +441517950148.

12 **ORCID ID:** 0000-0002-7399-8655

### 13 Abstract

14 Background. Evidence supports an important link between mitochondrial DNA (mtDNA) variation  
15 and adverse drug reactions such as idiosyncratic drug-induced liver injury (iDILI). Here we describe  
16 the generation of HepG2-derived transmitochondrial cybrids in order to investigate the impact of  
17 mtDNA variation upon mitochondrial (dys)function and susceptibility to iDILI against a constant  
18 nuclear background. In this study, cybrids were created to contain mitochondrial genotypes of  
19 haplogroup H and haplogroup J for comparison.

20 Methods. Briefly, HepG2 cells were depleted of mtDNA to make rho zero cells before the  
21 introduction of known mitochondrial genotypes using platelets from healthy volunteers (n=10), thus  
22 generating 10 distinct transmitochondrial cybrid cell lines. The mitochondrial function of each was  
23 assessed at basal state and following treatment with compounds associated with iDILI; flutamide, 2-  
24 hydroxyflutamide and tolcapone, by ATP assays and extracellular flux analysis.

25 Findings. Overall, baseline mitochondrial function was similar between haplogroups H and J.  
26 However, haplogroup specific responses to mitotoxic drugs were observed; haplogroup J was more  
27 susceptible to the inhibition of respiratory complexes I and II, and also to the effects of tolcapone, an  
28 uncoupler of mitochondrial respiration.

29 Conclusions. This study demonstrates that HepG2 transmitochondrial cybrids can be created to  
30 contain the mitochondrial genotype of any individual of interest, thus providing a practical and  
31 reproducible system to investigate the cellular consequences of variation in mitochondrial genome  
32 against a constant nuclear background. Additionally the results support that that inter-individual  
33 variation in mitochondrial genotype and haplogroup may be a factor in determining sensitivity to  
34 mitochondrial toxicants.

35 Funding. This work was supported by the Centre for Drug Safety Science supported by the Medical  
36 Research Council, United Kingdom (Grant Number G0700654); and GlaxoSmithKline as part of an  
37 MRC-CASE studentship (grant number MR/L006758/1).

38

## 39 Introduction

40

41 Drug-induced liver injury (DILI) is a leading cause of acute liver failure in the western world (Bernal  
42 and Wendon, 2013; Tujios and Lee, 2018). Although it is rare (19.1 cases per 100 000 inhabitants), it  
43 is a major cause of drug withdrawal due to its associated morbidity and mortality (Leise et al., 2014).  
44 Drug-induced liver injury can be broadly divided into two categories, idiosyncratic and intrinsic  
45 injury. Idiosyncratic DILI (iDILI) is characterised by a complex dose-response relationship, lack of  
46 predictivity from the primary pharmacology of a drug and significant interindividual variability. This  
47 means that despite being less common than intrinsic injury, iDILI can be viewed as far more costly  
48 (Fontana, 2014).

49 Drug-induced mitochondrial dysfunction is one of the mechanisms implicated in the onset of DILI,  
50 supported by the fact that 50% of drugs with a black box warning for hepatotoxicity also contain a  
51 mitochondrial liability, with many of these drugs associated specifically with iDILI (Dyken and Will,  
52 2007). It has been hypothesised that mitochondria is an important source of interindividual  
53 variation, underpinning susceptibility to iDILI. Specifically, mitochondria contain multiple copies of  
54 their own genome, mitochondrial DNA (mtDNA). Furthermore, single nucleotide polymorphisms  
55 (SNPs) in mtDNA are often inherited together forming mitochondrial haplogroups. Not only have  
56 associations between specific haplogroups and mitochondrial function been determined, but  
57 haplogroups have also been associated with specific adverse drug reactions and drug efficacy (Jones  
58 et al., 2021a).

59 The HepG2 cell line is one of the most commonly used preclinical cell lines for the *in vitro*  
60 assessment of DILI. However, this homogenous cell line does not encompass interindividual  
61 variation, including that of the mitochondrial genome. The importance of assessing the role of  
62 interindividual variation on patient susceptibility to adverse drug reactions is well recognised and  
63 the identification of mtDNA variants that confer susceptibility to iDILI could prove invaluable in drug  
64 development and drug safety. However, given the high economic cost associated with large,  
65 multicentre clinical trials, there is a need for new strategies enabling interindividual variation to be  
66 accounted for at the preclinical stage (Fermini et al., 2018; Jones et al., 2021b).

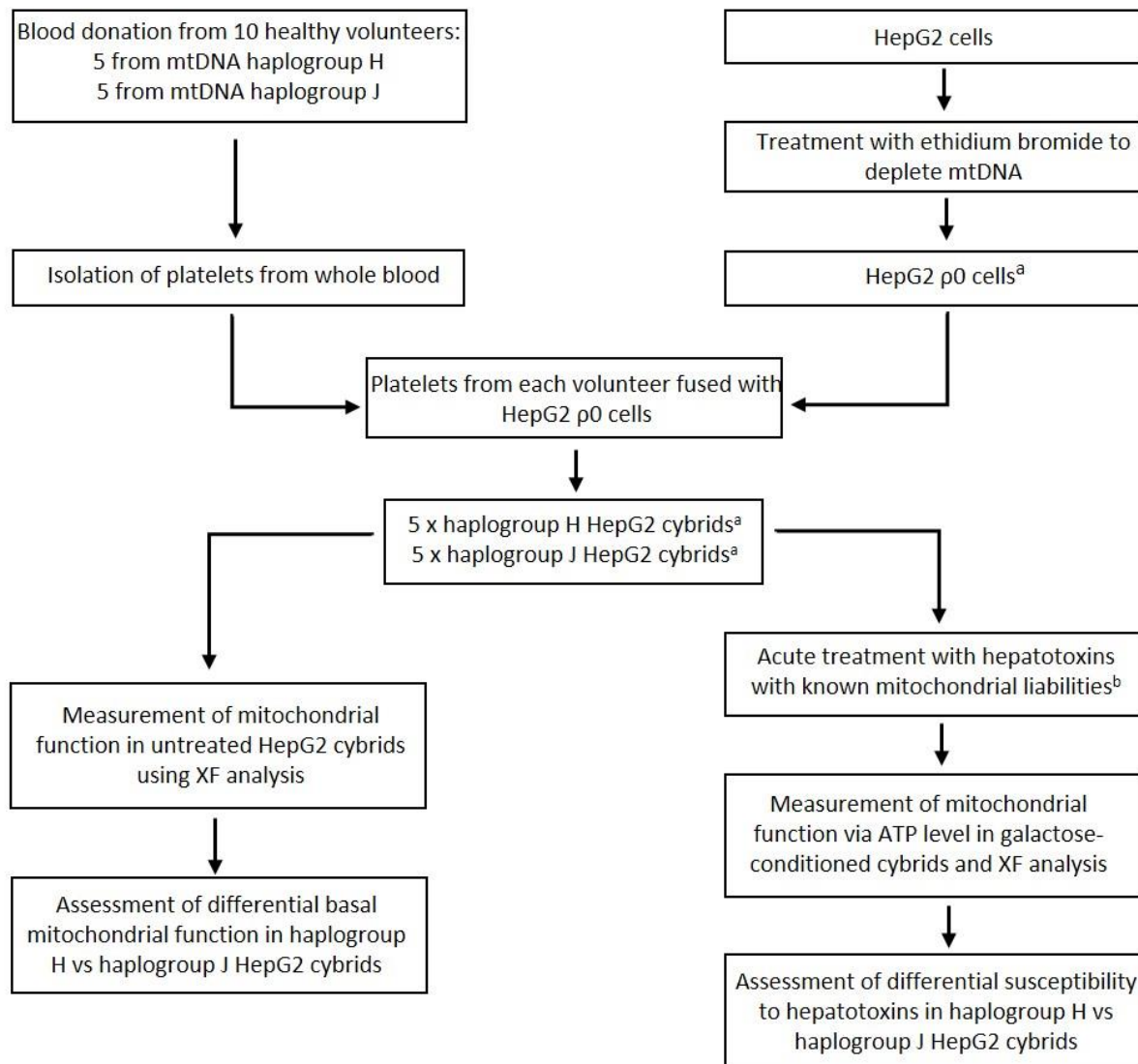
67 The generation of transmitochondrial cybrids enables mtDNA variation to be incorporated into  
68 reproducible *in vitro* models. Transmitochondrial cybrids are typically produced by the fusion of  
69 enucleated cells (cytoplasts) or anucleate cells (e.g. platelets) with cells that have been depleted of  
70 their mtDNA (rho zero [ $\rho 0$ ] cells) (King and Attardi, 1989). When cybrids are generated using the  
71 same population of  $\rho 0$  cells fused with anucleate cells harbouring different mtDNA variants, it is  
72 possible for the effects of mtDNA to be assessed against a stable nuclear background (Wilkins et al.,

73 2014; Penman et al., 2020). Excitingly, the representation of mtDNA variation using HepG2  
74 transmitochondrial cybrids may offer enhanced preclinical prediction of iDILI by facilitating the *in*  
75 *vitro* elucidation of the mechanistic basis of any differences associated with mtDNA variants, yet to-  
76 date there have been no reports of the generation of cybrids from a HepG2 p0 cell line (Bale et al.,  
77 2014).

78 Therefore, the overall aim of this study was to generate a panel of HepG2 transmitochondrial  
79 cybrids, as a proof of principle study, to investigate the effect of mtDNA variants upon mitochondrial  
80 function and their role, if any, in conferring susceptibility to drug-induced mitochondrial dysfunction.  
81 Specifically, ten populations of HepG2 transmitochondrial cybrids (herein referred to as cybrids)  
82 were created and characterised; five using platelets derived from healthy volunteers of haplogroup  
83 H and five from haplogroup J. Haplogroup H was selected as it is the most common haplogroup in  
84 the UK (Eupedia, 2016). Haplogroup J, on the other hand, is less common but is characterised by  
85 non-synonymous mutations in regions of the mitochondrial genome that encode mitochondrial  
86 respiratory complex I (Van Oven and Kayser, 2009; Eupedia, 2016). See Figure 1 for a schematic  
87 overview of the study.

88 Mitochondrial function was measured by ATP quantification in acutely galactose-conditioned cells,  
89 and extracellular flux (XF) analysis of both total respiratory chain function and the function of  
90 specific respiratory complexes, in whole and permeabilised cybrids, respectively. Drug-induced  
91 mitochondrial dysfunction was assessed by the treatment of cybrids with a panel of compounds  
92 selected to comprise of known hepatotoxins (a clinical association with DILI) with proven  
93 mitochondrial liabilities; flutamide, 2-hydroxyflutamide and tolcapone, alongside structural  
94 counterparts which are not hepatotoxic; bicalutamide and entacapone. Flutamide, a non-steroidal  
95 antiandrogen for the treatment of prostate cancer has a boxed warning for hepatotoxicity and is a  
96 known inhibitor of mitochondrial complex I (Coe et al., 2007). 2-hydroxyflutamide, is the primary  
97 metabolite of flutamide and is a known inhibitor of both respiratory complex I and respiratory  
98 complex II. In humans, the rapid first-pass metabolism of flutamide results in 2-hydroxyflutamide  
99 having a much higher maximum serum concentration than its parent compound (4400 nM versus  
100 72.2 nM). However, HepG2 cells have limited expression of many enzymes required for xenobiotic  
101 metabolism, including cytochrome P450 1A2, the primary route of flutamide metabolism to  
102 generate 2-hydroxyflutamide; therefore cybrids were also dosed with 2-hydroxyflutamide directly  
103 (Shet et al., 1997; Sison-Young et al., 2015; Ball et al., 2016). Tolcapone, a catechol-o-methyl  
104 transferase inhibitor used to treat Parkinson's disease was withdrawn due to cases of liver failure  
105 and is a known uncoupler of oxidative phosphorylation (Olanow, 2000; Benabou and Waters, 2003;  
106 Olanow and Watkins, 2007).





108

109 **Figure 1 Study Overview.**

110 <sup>a</sup> HepG2 ρ0 cells were characterised to ensure the complete depletion of mtDNA and HepG2 cybrids were  
111 characterised to ensure the expression of mtDNA-encoded proteins. Methods of characterisation are  
112 described in the Supplementary Information.

113 <sup>b</sup> Flutamide, 2-hydroxyflutamide and tolcapone, alongside non-hepatotoxic structural counterparts;  
114 bicalutamide and entacapone.

115 Abbreviations: Abbreviations: mtDNA, mitochondrial DNA; ρ0, rho zero; XF, extracellular flux.

116

117 Results

118 *Haplogroup J cybrids have greater respiratory complex activity than haplogroup H cybrids*

119 Assessment of basal mitochondrial function using a mitochondrial stress test showed no significant  
120 difference between haplogroup H and J cybrids in multiple parameters of mitochondrial respiration  
121 (Figure 2A). Contrastingly, haplogroup J cybrids had significantly greater ( $\geq 2$  fold;  $p=0.025$ ,  $p=0.001$ )  
122 complex I and II-driven maximal respiration (herein referred to as complex activity for clarity)  
123 (Figure 2B).

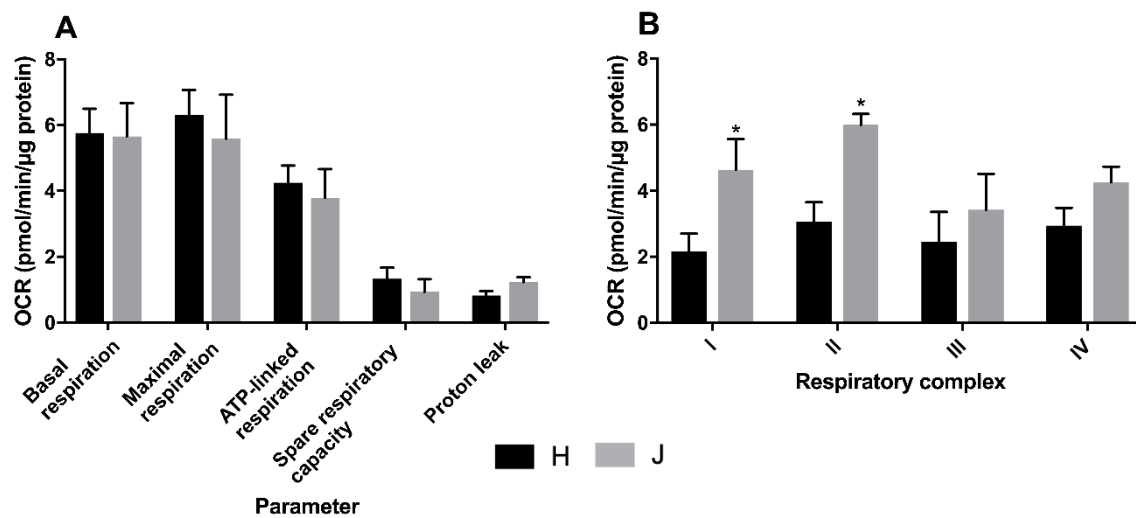


**Figure 2 Basal mitochondrial function and respiratory complex activity in haplogroup H and J HepG2 cybrids.**

**A:** Untreated haplogroup H and J cybrids were assessed using extracellular flux analysis and a mitochondrial stress test to measure: basal respiration, maximal respiration, ATP-linked respiration, spare respiratory capacity and proton leak.

**B:** Untreated haplogroup H and J cybrids were assessed using extracellular flux analysis and respiration was stimulated by the supply of respiratory complex-specific substrates. Complex I-IV activity was defined as complex I-IV driven maximal respiration. Statistical significance between haplogroup H and J cybrids: \*  $p < 0.05$ . Data are presented as mean + SEM of  $n=5$  experiments. Abbreviations: OCR, oxygen consumption rate. Source data: fig2 – source data file.xlsx

124

125 *Inhibition of mitochondrial respiration by flutamide is similar in haplogroup H and J cybrids*

126 Acute treatment of galactose-conditioned cybrids with flutamide did not induce cytotoxicity (i.e. no  
 127 significant lactate dehydrogenase [LDH] release) at any of the concentrations used (data not shown).  
 128 A substantial, concentration-dependent decrease in ATP was evident when cybrids were treated  
 129 with  $\geq 33 \mu\text{M}$  flutamide, but the decrease was not significantly different between haplogroup H and J  
 130 cybrids (Figure 3A). Concordantly, there was no significant difference in the ATP level  $\text{EC}_{50}$  between  
 131 the two haplogroups. XF analysis also revealed no significant difference in parameters of  
 132 mitochondrial respiration between haplogroup H and haplogroup J cybrids when treated with  
 133 flutamide, though haplogroup J cybrids did have a greater proton leak and reduced spare respiratory

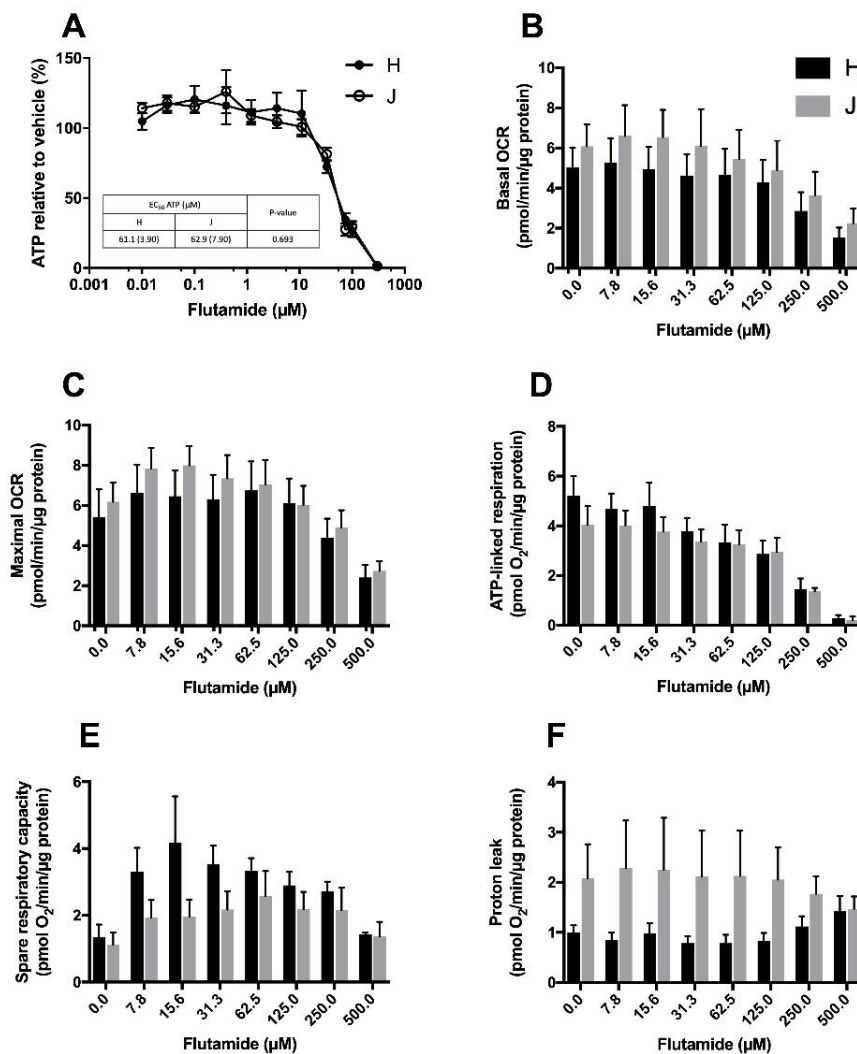


**Figure 3** The effect of flutamide upon ATP levels and mitochondrial respiratory function in haplogroup H and J HepG2 cybrids. A: Cybrids were treated (2 h) with up to 300  $\mu\text{M}$  flutamide in galactose medium. ATP values are expressed as a percentage of those of the vehicle control. B-F: Changes in basal respiration, maximal respiration, ATP-linked respiration, spare respiratory capacity and proton leak following acute treatment with flutamide (up to 500  $\mu\text{M}$ ). Data are presented as mean  $\pm$  SEM of  $n=5$  experiments. Abbreviations: OCR, oxygen consumption rate. Source data: fig3 – source data file.xlsx



134 capacity than haplogroup H at all concentrations, but this was not significant (Figure 3B-F).

135 *Inhibition of mitochondrial respiration by 2-hydroxyflutamide is similar in haplogroup H and J cybrids*

136 Acute treatment of galactose-conditioned cybrids with 2-hydroxyflutamide did not induce  
 137 cytotoxicity at any of the concentrations used (data not shown). A substantial, concentration-  
 138 dependent decrease in ATP level was evident when cybrids were treated with  $\geq 33 \mu\text{M}$  2-  
 139 hydroxyflutamide, but the decrease was not significantly different between haplogroup H and J  
 140 cybrids at any single concentration (Figure 4A); however, a comparison of  $\text{EC}_{50}$  values showed a  
 141 small but significantly lower  $\text{EC}_{50}$  value in haplogroup H cybrids (Figure 4A;  $p=0.003$ ). XF analysis also  
 142 revealed no significant difference in parameters of mitochondrial respiration between haplogroup H  
 143 and haplogroup J cybrids when treated with 2-hydroxyflutamide (Figure 4B-F). As was the case with  
 144 flutamide, 2-hydroxyflutamide-treated haplogroup J cybrids had a greater proton leak and reduced  
 145 spare respiratory capacity compared with haplogroup H at most concentrations, but this was not

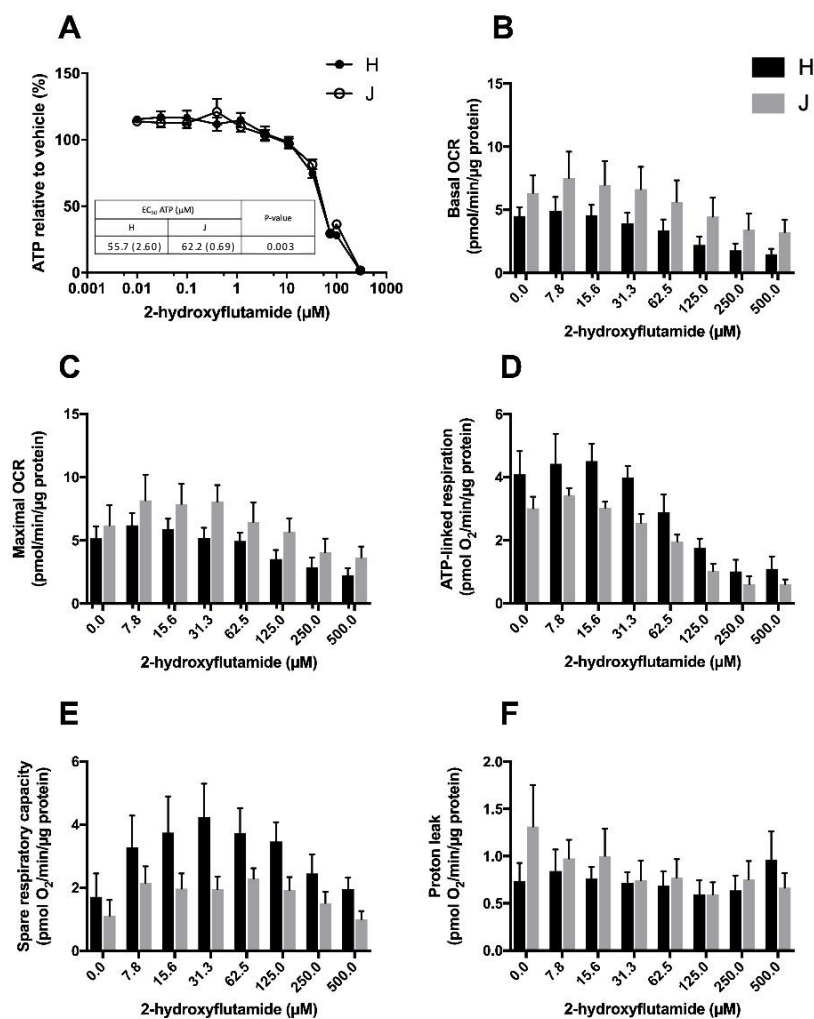


**Figure 4** The effect of 2-hydroxyflutamide upon ATP levels and mitochondrial respiratory function in haplogroup H and J HepG2 cybrids. **A:** Cybrids were treated (2 h) with up to 300  $\mu\text{M}$  2-hydroxyflutamide in galactose medium. ATP values are expressed as a percentage of those of the vehicle control. **B-F:** Changes in basal respiration, maximal respiration, ATP-linked respiration, spare respiratory capacity and proton leak following acute treatment with 2-hydroxyflutamide (up to 500  $\mu\text{M}$ ). Data are presented as mean  $\pm$  SEM of  $n=5$  experiments. Abbreviations: OCR, oxygen consumption rate. Source data: fig4 – source data file.xlsx

146 significant (Figure 4E, F).

147 *Haplogroup H cybrids are resistant to tolcapone-induced ATP depletion at <75 μM*

148 Cellular ATP levels following treatment with up to 75 μM tolcapone were significantly higher in  
 149 haplogroup H cybrids; this was reflected by the significantly higher EC<sub>50</sub> in haplogroup H cybrids,  
 150 almost twice that of haplogroup J (Figure 5A; p<0.0001). At higher concentrations of tolcapone  
 151 however, there was no significant difference between the two haplogroups (Figure 5A). XF analysis  
 152 showed no significant difference in parameters of mitochondrial respiration between haplogroup H  
 153 and haplogroup J cybrids when treated with tolcapone (Figure 5B-F).

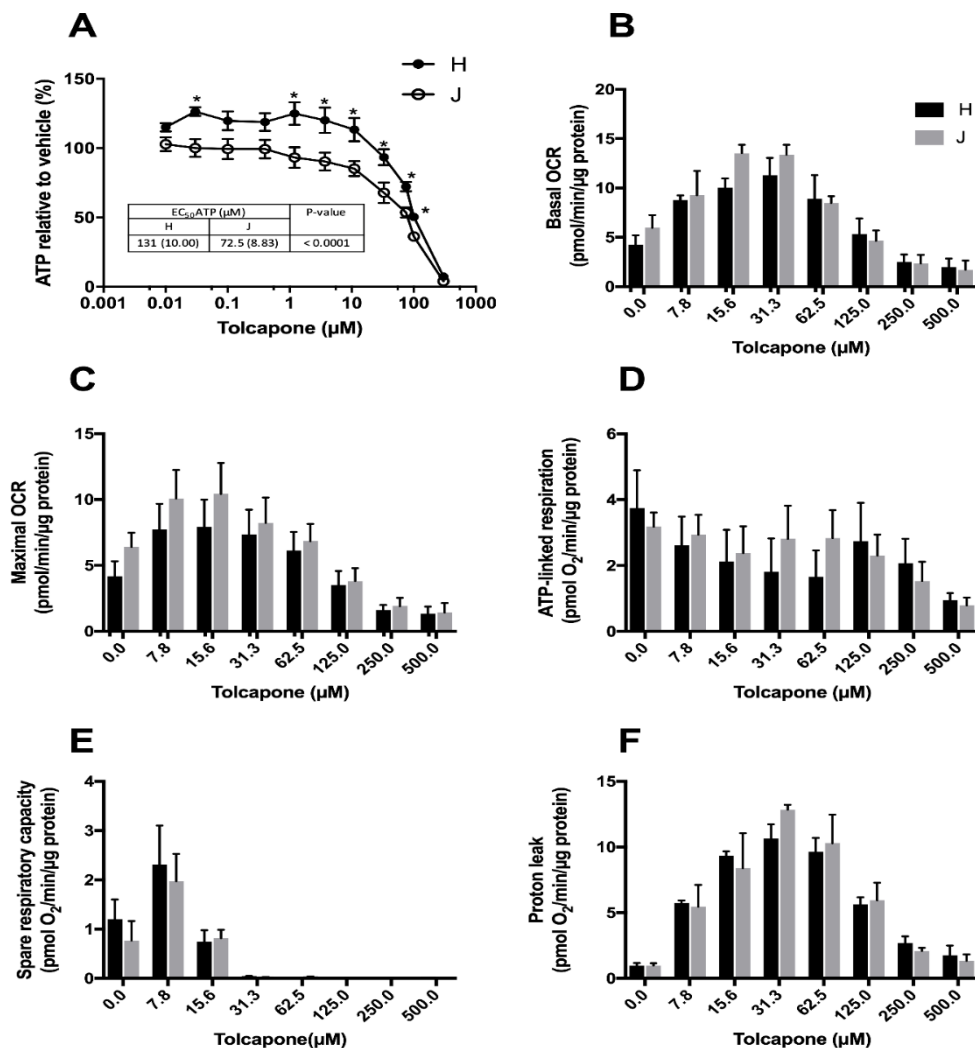


**Figure 5** The effect of tolcapone upon ATP levels and mitochondrial respiratory function in haplogroup H and J HepG2 cybrids. **A:** Cybrids were treated (2 h) with up to 300 μM tolcapone in galactose medium. ATP values are expressed as a percentage of those of the vehicle control. **B-F:** Changes in basal respiration, maximal respiration, ATP-linked respiration, spare respiratory capacity and proton leak following acute treatment with tolcapone (up to 500 μM). Statistical significance between : haplogroup H and J cybrids\* p<0.05. Data are presented as mean ± SEM of n=5 experiments. Abbreviations: OCR, oxygen consumption rate. Source data: fig 5 – source data file.xlsx



155 *Haplogroup J cybrids have greater respiratory complex activity but are more susceptible to inhibition of*  
156 *complex I and II activity by flutamide and 2-hydroxyflutamide*

157 When treated with flutamide (complex I inhibitor) haplogroup J cybrids had significantly greater  
158 respiratory complex I/II activity at all but the highest flutamide concentration (250  $\mu$ M), peaking at  
159 approximately two-fold greater activity than haplogroup H cybrids (Figure 6A, B). Though complex I  
160 activity was greater in haplogroup J cybrids at all concentrations, haplogroup J cybrids exhibited a  
161 bigger decrease (compared with haplogroup H cybrids) in complex I activity relative to control when  
162 treated with flutamide (Figure 6A). The effect of treatment with 2-hydroxyflutamide mirrored the  
163 effect of its parent compound, flutamide, with greater complex I activity in haplogroup J cybrids at  
164 all concentrations, but with haplogroup J cybrids exhibiting the biggest decrease in complex I activity  
165 relative to control (Figure 6C).

166 A smaller difference was observed in complex II activity between the two cybrid haplogroups when  
167 treated with 2-hydroxyflutamide, though greater activity was still evident in haplogroup J cybrids at  
168 all concentrations (Figure 6D).

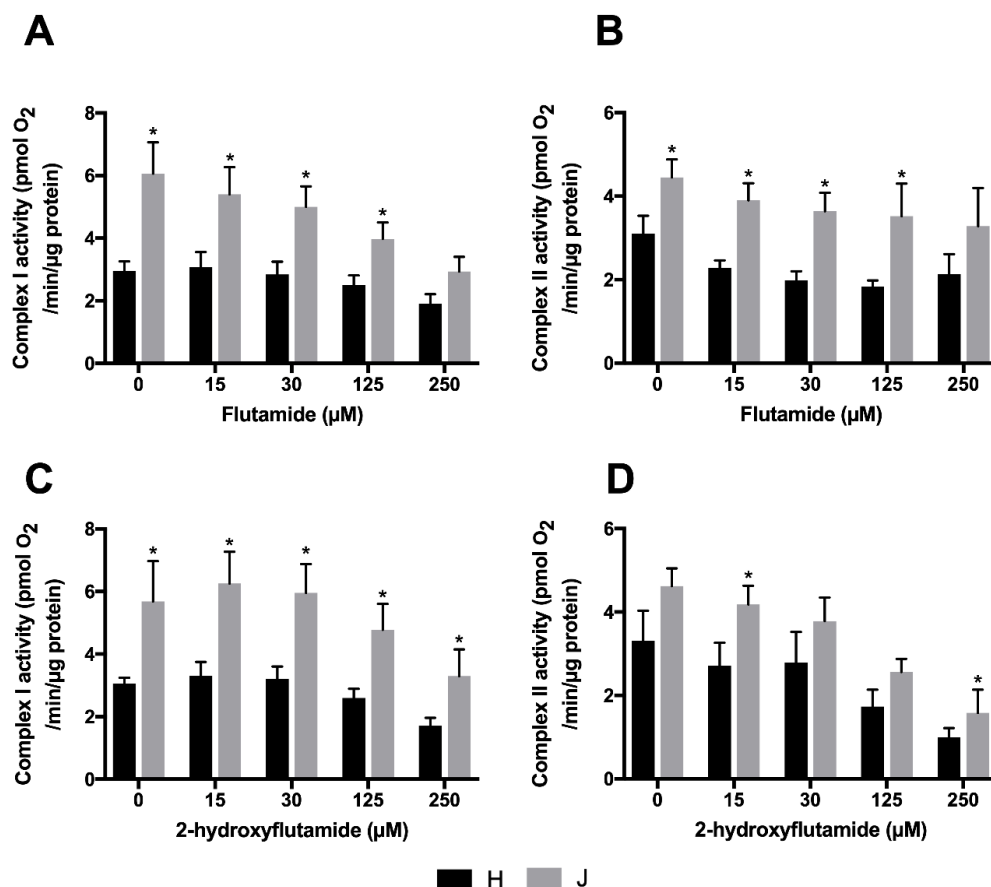


Figure 6 The effect of flutamide and 2-hydroxyflutamide upon respiratory complex I and II in haplogroup H and J HepG2 cybrids. Permeabilised cybrids were acutely treated with flutamide (A, B) or 2-hydroxyflutamide (C, D) ( $\leq$ 250  $\mu$ M) before a mitochondrial stress test using extracellular flux analysis. Complex I/II activity was defined as complex I/II driven maximal respiration. Statistical significance between haplogroup H and J cybrids: \*  $p < 0.05$ . Data are presented as mean + SEM of  $n=5$  experiments. Source data: fig 6 – source data file.xlsx

169

170 *The impact of bicalutamide and entacapone on mitochondrial respiration and ATP levels is similar in*  
171 *haplogroup H and J cybrids*

172 When treated with bicalutamide and entacapone (non-hepatotoxic structural counterparts of  
173 flutamide and tolcapone, respectively), the effect on mitochondrial respiration and ATP levels was  
174 similar in haplogroup H and J cybrids. Full results are described in the Supplementary Information.

175 Discussion

176

177 It has been widely hypothesised that individual variation in mtDNA may be a factor underlying the  
178 onset of idiosyncratic adverse drug reactions by drugs known to contain mitochondrial liabilities.  
179 Evidence from clinical studies has demonstrated that such associations between mitochondrial  
180 genotype and drug efficacy or adverse events do exist (Jones et al., 2021a). However, there is a lack  
181 of knowledge and understanding of the importance of these findings due to the presence of nuclear  
182 heterogeneity alongside environmental factors in clinical cohorts and the small size of test cohorts,  
183 as well as historical limitations in sequencing technology. Because of this we have created a  
184 transmitochondrial cybrid cell panel, in which mitochondria of known genotype, sourced from  
185 volunteer platelets, were inserted into HepG2 p0 cells in order to produce a “personalised model”  
186 model of mitotoxicity suitable for mechanistic investigations.

187 Here we describe the successful generation of 10 distinct transmitochondrial cybrid cell lines,  
188 derived from five haplogroup H volunteers and five haplogroup J volunteers. To the best of our  
189 knowledge, this is the first time that the creation of a panel of HepG2-derived transmitochondrial  
190 cybrids has been reported. Importantly, the HepG2 cell line is one of the most commonly used cell  
191 lines in preclinical drug safety testing and therefore the HepG2 cybrids generated in the present  
192 study are of great value in improving the understanding of iDILI by providing an *in vitro*  
193 representation of the interindividual variation that underpins this adverse drug reaction (Bale et al.,  
194 2014). In this work, the utility of these cells to investigate interhaplogroup differences in  
195 mitochondrial function has been demonstrated, with HepG2 cybrids of haplogroup J displaying  
196 greater mitochondrial respiratory complex activity at basal state. Moreover, our investigations  
197 revealed that there were haplogroup-specific differences in susceptibility to hepatotoxic compounds  
198 that target the electron transport chain (ETC). Specifically, haplogroup J cybrids were more  
199 susceptible to: a reduction in respiratory complex I activity induced by flutamide, a reduction in  
200 respiratory complex I and II activity induced by 2-hydroxyflutamide, and a reduction in ATP levels  
201 induced by tolcapone.

202 The methodology developed for the generation of HepG2 cybrids has enabled the creation of a  
203 HepG2 cybrid cell panel from two of the most common mitochondrial haplogroups in England, H and  
204 J; which account for more than 50% of the population (Eupedia, 2016). Although baseline  
205 assessments revealed only marginal differences in mitochondrial function between haplogroup H  
206 and J cybrids, the recruitment of healthy volunteers for this study (i.e. no clinical phenotype of  
207 mitochondrial dysfunction), meant that the absence of any substantial differences in mitochondrial  
208 function was expected. This recruitment of healthy volunteers is representative of the clinical  
209 situation, as individuals who experience iDILI tend not to display a phenotype of mitochondrial  
210 dysfunction prior to treatment. Additionally, it should be noted that these results were analysed on  
211 the basis of macro-haplogroup (i.e H, J). However, each cybrid cell line has been identified as a  
212 separate sub-haplogroup (e.g. H1, J2), based upon the accumulation of specific SNPs (see  
213 Supplementary Information). This lack of homogeneity within the test groups may mask  
214 associations.

215 The cybrid cell panel was interrogated using known drug mitotoxicants which elicit different effects  
216 on the ETC; flutamide and 2-hydroxyflutamide, direct ETC inhibitors, and tolcapone, an ETC  
217 uncoupler. The impact of flutamide (complex I inhibitor) and 2-hydroxyflutamide (complex I and II  
218 inhibitor) upon cellular ATP level was similar between haplogroup H and J cybrids. However,  
219 haplogroup H cybrids exhibited a degree of resistance to ATP depletion induced by tolcapone; a  
220 resistance that was not observed in haplogroup J cybrids. This agrees with findings reported by  
221 Ghelli *et al.*, 2009 in which a cybrid model (non-hepatic) was used to determine that haplogroup J (vs  
222 haplogroups H and U) was more susceptible to uncoupling by the neurotoxic metabolite, 2,5-  
223 hexanediol (Ghelli *et al.*, 2009). When assessing the relevance of the results from the present study,  
224 it is important to note that test concentrations were selected in order to generate the maximum  
225 effect on mitochondrial function in the absence of toxicity. The authors recognise that higher  
226 concentrations were used than  $C_{max}$  of compounds, however the goal was to model the  
227 mitochondrial toxicity experienced in a small number of individuals, which was not possible at lower  
228 concentrations. It is important to note that there was a lack of these described haplogroup-specific  
229 effects when using the non-hepatotoxic counterparts of the test compounds, bicalutamide and  
230 entacapone, illustrating that any differences are mechanisms- via induced mitochondria dysfunction.

231 Further analysis of the effects of the compounds upon respiration showed that the impact of  
232 flutamide and 2-hydroxyflutamide on parameters of mitochondrial respiration was similar between  
233 haplogroup H and J, though haplogroup J cybrids had consistently higher rates of respiration.  
234 Parameters of mitochondrial respiration also remained similar between the two cybrid haplogroups  
235 upon treatment with tolcapone. Given that the ATP level of cells, and indeed overall respiration, is

236 the product of a myriad of processes to maintain energy status, mitochondrial function was  
237 dissected further by assessing the basal activity of specific respiratory complexes. Despite marginal  
238 differences in overall basal mitochondrial respiration, the basal activity of specific respiratory  
239 complexes showed significantly higher complex I and II activity in haplogroup J compared with  
240 haplogroup H cybrids. However, haplogroup J cybrids also displayed a heightened susceptibility to  
241 inhibition of complex I and II activity by flutamide/2-hydroxyflutamide. In contrast to complex I,  
242 complex II is entirely encoded in the nuclear genome, therefore one might predict that this should  
243 not differ between mitochondrial haplogroups. Nonetheless, upon the introduction of the foreign  
244 mitochondrial genome into cybrids, the initiation of retrograde responses to the nucleus must  
245 ensue, primarily via calcium signalling, which would enable regulation of the nuclear-encoded  
246 mitochondrial proteome and potentially enhanced biogenesis of respiratory complexes in  
247 haplogroup J (Luo et al., 1997; Amuthan et al., 2002; Srinivasan et al., 2015). This mechanism could  
248 account for the observed differential complex II activity.

249 The finding that haplogroup H cybrids are more resistant to ATP depletion induced by tolcapone  
250 offers new insights into the potential mechanisms underlying the onset of iDILI in certain individuals.  
251 In the case of tolcapone, four instances of liver failure among the 100 000 individuals who were  
252 administered the drug led to a black box warning and a switch in use to an alternative in-class  
253 compound, entacapone. However, as entacapone has been reported to be less efficacious than  
254 tolcapone, the ability to stratify therapy based upon the risk of iDILI, would be of great value (Rivest  
255 et al., 1999; Olanow, 2000; Watkins, 2000; Benabou and Waters, 2003; Olanow and Watkins, 2007;  
256 Lees, 2008; Longo et al., 2016).

257 Overall, this research offers insights into the potential importance of mitochondrial haplogroup on  
258 drug-induced mitochondrial dysfunction and iDILI. In the present study, HepG2 cybrids have been  
259 generated from only two mitochondrial haplogroups due to sample size limitations, but the method  
260 established offers itself to the generation of HepG2 cybrids from volunteers of other mitochondrial  
261 haplogroups and also from volunteers who are identical at the level of subhaplogroup. Furthermore,  
262 it is of note that differences in susceptibility have been observed despite the division of cybrids into  
263 two haplogroups which encompass much variation, and suggests that the comparison of more  
264 homogenous mtDNA subhaplogroups may provide further, more valuable insights into the  
265 differences conferred by differential mitochondrial background.

266

267 In conclusion, this study has established a novel, *in vitro* model that provides a preclinical  
268 representation of interindividual variation underpinning iDILI, thereby offering much greater  
269 translatability to clinical scenarios compared with current, homogenous preclinical models. This is

270 paramount in understanding the safety of a drug in a range of populations prior to clinical trials, thus  
271 improving patient safety, as well as reducing drug attrition.

## 272 **Materials and Methods**

### 273 *Materials*

274 All forms of DMEM were purchased from Life Technologies (Paisley, UK). HepG2 cells were  
275 purchased from European Collection of Cell Cultures (Salisbury, UK). Cytotoxicity detection kits were  
276 purchased from Roche Diagnostics Ltd (West Sussex, UK). Clear and white 96-well plates were  
277 purchased from Fisher Scientific (Loughborough, UK) and Greiner Bio-One (Stonehouse, UK)  
278 respectively. All XF assay consumables were purchased from Agilent Technologies (CA, USA). All  
279 other reagents and chemicals were purchased from Sigma Aldrich (Dorset, UK) unless otherwise  
280 stated.

### 281 *Cohort*

282 Ten healthy volunteers were recalled to give blood from the previously established HLA-typed  
283 archive (Alfirevic et al. 2012). These volunteers were selected upon the basis of their mitochondrial  
284 haplogroup (haplogroup H and J) and this genotyping has been described in our previous publication  
285 (Ball *et al*, 2021). Mitochondrial subhaplogroups and SNPs of the DNA isolated from each individual  
286 are described in the Supplementary Information. Ten donors were selected as an adequate number  
287 for a proof of principle study on the feasibility of generating the transmitochondrial cybrids. The  
288 volunteers were eligible to take part in the study if they were aged between 18 and 60 years,  
289 healthy and willing to donate one or more blood samples. The following exclusion criteria were  
290 applied and volunteers were not recruited if: they donated blood to transfusion services in the last 4  
291 months; they had any medical problems, including asthma, diabetes, epilepsy or anemia; on any  
292 medications or if they had taken any recreational drugs in the last 6 weeks (including cannabis,  
293 speed, ecstasy, cocaine, LSD, and so on). Women were excluded if pregnant. This project was  
294 approved by the North West of England Research Ethics Committee and all participants gave written  
295 informed consent. Volunteer confidentiality was maintained by double coding DNA samples and by  
296 restricting access to participant's personal data to trained clinical personnel. Detailed study eligibility  
297 and exclusion criteria have been published previously (Alfirevic et al. 2012).

298

### 299 *Generation of HepG2 cybrids*

#### 300 *Generation of HepG2 p0 cells*

301 HepG2 cells (ECACC Cat# 85011430, RRID:CVCL\_0027) ( $\leq$  passage 7) were cultured and passaged as  
302 required in HepG2 p0 cell medium (DMEM/F-12 +GlutaMAX™ supplemented with FBS [10% v/v],  
303 L-glutamine [4 mM], sodium pyruvate [1 mM], HEPES [2 mM] and uridine [500  $\mu$ M]) in the presence



304 of ethidium bromide (EtBr; 1  $\mu$ M). During treatment with EtBr (1  $\mu$ M), the chemical was removed for  
305 48 h every two weeks to help maintain cell viability. Following eight weeks' exposure, EtBr was  
306 removed from a subset of cells for one week prior to characterisation to ensure cells were devoid of  
307 mtDNA i.e. were  $\rho$ 0 cells (see Supplementary Information). If a  $\rho$ 0 cell phenotype was not evident,  
308 cells were returned to EtBr treatment (1  $\mu$ M) prior to removal for another week and re-testing, until  
309 a  $\rho$ 0 cell population was observed.

#### 310 Platelet isolation

311 Healthy volunteers, five of mitochondrial haplogroup H, and five of haplogroup J, donated whole  
312 blood from which platelets were isolated according to methods previously described (Ball et al.,  
313 2021). Briefly, 50 mL of blood was donated by each volunteer, and this fresh whole blood was  
314 immediately processed by a series of density centrifugation steps to produce isolated platelets.  
315 Throughout the procedure, PGI<sub>2</sub> was used (1  $\mu$ g/mL) to prevent platelet activation.

#### 316 Platelet fusion with HepG2 rho zero ( $\rho$ 0) cells

317 During the final centrifugation step of platelet isolation, HepG2  $\rho$ 0 cells were collected by  
318 trypsinisation and resuspended in HepG2  $\rho$ 0 cell medium. Following cell viability assessment (trypan  
319 blue; all viabilities were recorded at >90%),  $\rho$ 0 cells ( $6 \times 10^6$  cells) were centrifuged (1000 g, 5 min)  
320 and resuspended in Ca<sup>2+</sup>-free DMEM (2 mL; supplemented with 1 mM PGI<sub>2</sub>). This cell suspension  
321 was added to isolated platelets using a Pasteur pipette so as to minimise disruption to the platelet  
322 pellet. The cell mixture was then centrifuged (180 g, no brake, 10 min) to form a multi-layered pellet  
323 of platelets and HepG2  $\rho$ 0 cells.

324 Following centrifugation, the supernatant was removed and polyethylene glycol (250  $\mu$ L; PEG 50%)  
325 was added before resuspending the cell pellet (30 s) followed by a 1 min incubation period. At the  
326 end of the incubation period, HepG2  $\rho$ 0 cell medium (30 mL) was added and a further 10-fold or 2-  
327 fold dilution with HepG2  $\rho$ 0 cell medium was performed before seeding into 96-well, 12-well and 6-  
328 well plates (Figure 7)

329

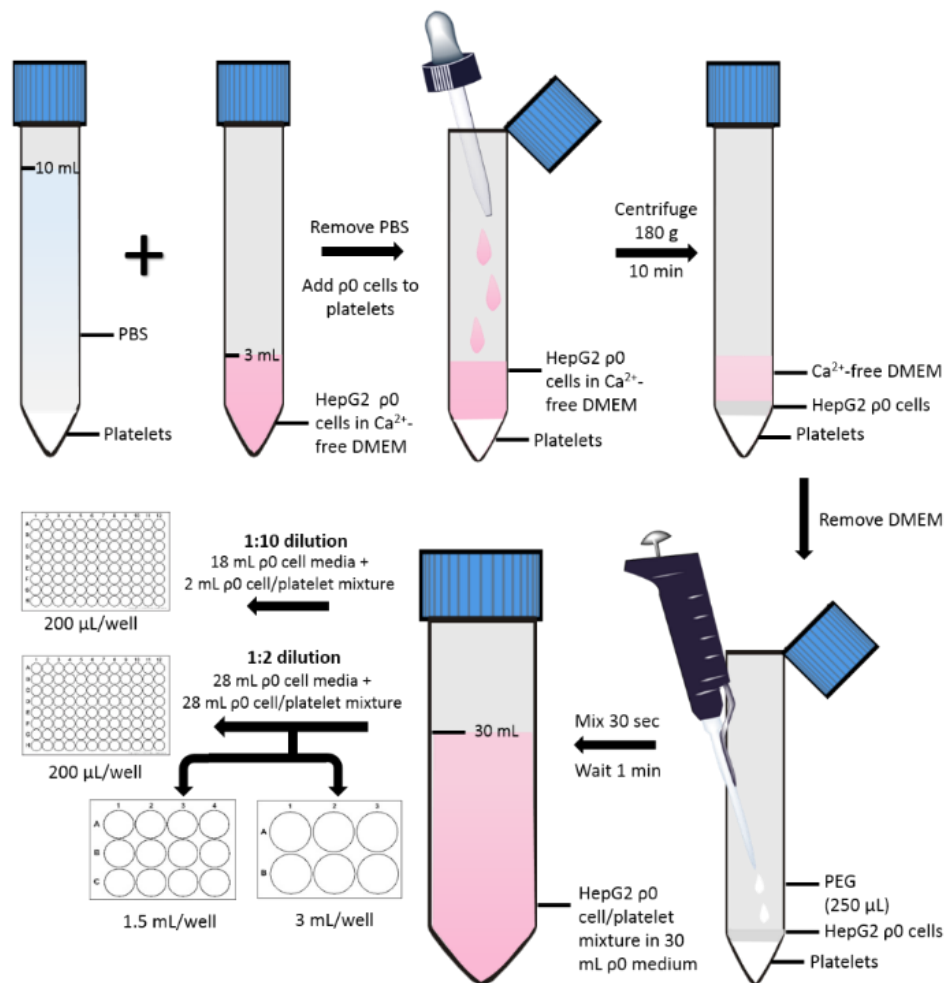


**Figure 7 Schematic representation of the fusion of HepG2 p0 cells and platelets to generate HepG2 transmittochondrial cybrids.** HepG2 p0 cells were assessed for viability (trypan blue; all viabilities were recorded at >90%),  $6 \times 10^6$  p0 cells were then centrifuged (1000 g, 5 min) and resuspended in Ca<sup>2+</sup>-free DMEM (2 mL; supplemented with 1 mM PGI<sub>2</sub>). This cell suspension was added to isolated platelets using a Pasteur pipette so as to minimise disruption to the platelet pellet. The cell mixture was then centrifuged (180 g, no brake, 10 min) to form a multi-layered pellet of platelets and HepG2 p0 cells. Following centrifugation, the supernatant was removed and polyethylene glycol (250 μL; PEG 50%) was added before resuspending the cell pellet (30 sec) followed by a 1 min incubation period. At the end of the incubation period, HepG2 p0 cell medium (30 mL) was added and a further 10-fold or 2-fold dilution with HepG2 p0 cell medium was performed before seeding into 96-well, 12-well and 6-well plates. Abbreviations: PEG, polyethylene glycol; p0, rho zero.

330 Two days post-fusion, media were replaced with fresh HepG2 p0 cell medium. After a further two  
 331 days, this was replaced with medium consisting of equal volumes of HepG2 p0 medium and cybrid  
 332 selection medium (high-glucose DMEM [glucose; 25 mM] supplemented with dialysed FBS [10% v/v],  
 333 amphotericin B [1.35 μM] and antibiotic/antimycotic solution [100 units penicillin/mL, 170 μM  
 334 streptomycin and 270 nM amphotericin B]). Finally, two days later, media were switched to 100%  
 335 cybrid selection medium. p0 cells are auxotrophic for pyruvate and uridine, so the absence of these  
 336 two constituents was the basis for the selection of successfully fused cells i.e. HepG2 cybrids. Cells

337 remaining after selection were characterised to ensure a HepG2 cybrid phenotype by measuring the  
338 expression and function of mtDNA-encoded proteins (see Supplementary Information). Cells were  
339 then cultured and passaged as required in cybrid maintenance medium (DMEM high-glucose  
340 supplemented with FBS [10% v/v], L-glutamine [4 mM], sodium pyruvate [1 mM] and HEPES [1  
341 mM]). For a schematic representation of HepG2 cybrid generation see Figure 8.  
342

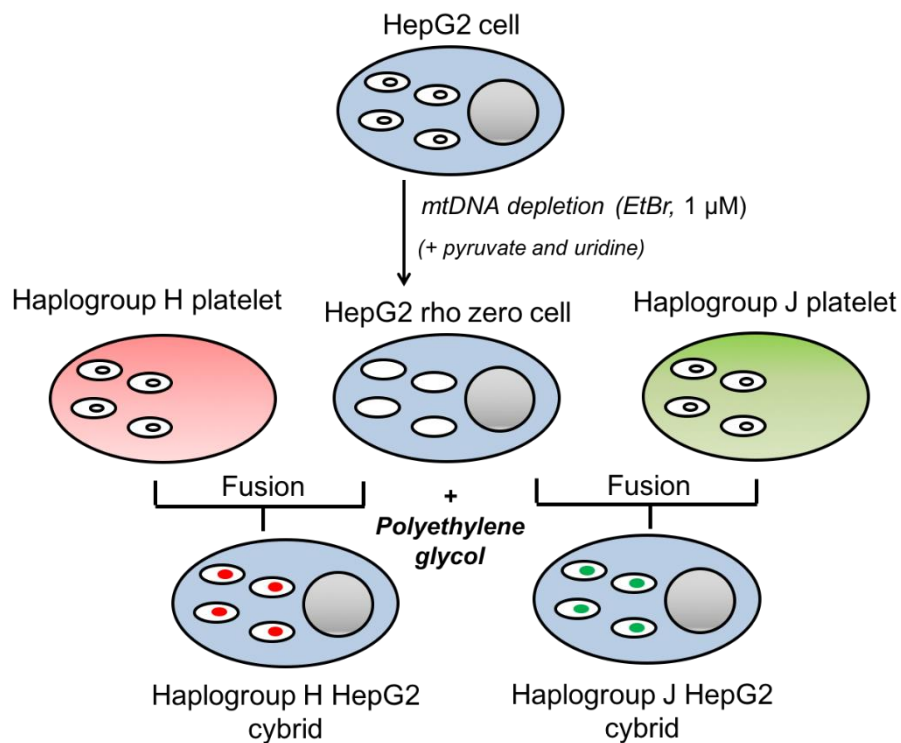


**Figure 8 Schematic representation of HepG2 transmittochondrial cybrid generation.** HepG2 cells were cultured in the presence of 1 μM ethidium bromide to generate HepG2 ρ0 cells. HepG2 ρ0 cells were combined with freshly-isolated platelets from healthy volunteers of mitochondrial haplogroup H or J and centrifuged (180 g, 10 min) to generate a multi-layered pellet. Following removal of the supernatant, polyethylene glycol (PEG; fusion reagent) was added and suspended with the cell mixture. After incubation with PEG for 1 min, 30 mL of HepG2 ρ0 cell medium was added (containing uridine and pyruvate) before further dilutions into a range of cell culture vessel sizes. This cell mixture was then cultured in cybrid selection medium (devoid of pyruvate and uridine), remaining cells were characterised to ensure the expression and function of mtDNA-encoded proteins. Abbreviations: EtBr, ethidium bromide; mtDNA, mitochondrial DNA.

343

344 *Assessment of mitochondrial function at basal state and following incubation with flutamide, 2-*  
345 *hydroxyflutamide and tolcapone*

346 *Dual assessment of mitochondrial function (ATP content) alongside cytotoxicity (LDH release)*

347 *Cell and reagent preparation*

348 HepG2 cybrids were collected by trypsinisation and seeded on a collagen-coated flat-bottomed  
349 96-well plate in cybrid maintenance medium (20 000 cells/50 µL/well) and incubated (24 h, 37°C, 5%  
350 CO<sub>2</sub>). Cells were then washed three times in serum-free galactose medium (DMEM containing 10  
351 mM galactose and 6 mM L-glutamine) before addition of galactose medium (50 µL) and further  
352 incubation (2 h, 37°C, 5% CO<sub>2</sub>). This acute metabolic modification has been shown to be sufficient to  
353 allow the identification of drugs which induce mitochondrial dysfunction, by reducing the ATP yield  
354 from glycolysis, thereby increasing reliance on OXPHOS for ATP production. Flutamide, 2-  
355 hydroxyflutamide, tolcapone, bicalutamide and entacapone were each serially diluted to generate a  
356 concentration range of 0.01 – 300 µM in galactose medium. Diluted compounds (50 µL) were then  
357 added to each well (total well volume; 100 µL) and cells were incubated (2 h, 37°C, 5% CO<sub>2</sub>) before  
358 conducting assays to assess mitochondrial function and cytotoxicity. All assays used ≤0.5% DMSO as  
359 a vehicle control.

360 *ATP content assay*

361 ATP content was assessed by the addition of cell lysate (10 µL) and ATP standard curve solutions to a  
362 white-walled 96-well plate. ATP assay mix (40 µL; prepared according to the manufacturer's  
363 instructions) was then added and bioluminescence was measured (Varioskan, Thermo Scientific).

364 *LDH release assay*

365 LDH release was determined by the extraction of 25 µL supernatant and 10 µL cell lysate from each  
366 well, before use of a cytotoxicity detection kit and reading at 490 nm. LDH release was calculated as:  
367 LDH supernatant/ (supernatant + lysate).

368 *Normalisation (BCA assay)*

369 Protein content was determined using cell lysate (10 µL) and protein standards (10 µL). BCA assay  
370 fluorescence was then measured at 570 nm.

371 *Extracellular flux analysis*

372 HepG2 cybrids were collected by trypsinisation and seeded on a collagen-coated XFe96 cell culture  
373 microplate (25 000 cells/100 µL medium/well; 96-well plate) and incubated (37°C, 5% CO<sub>2</sub>)  
374 overnight.

375 *Mitochondrial stress test*

376 Please refer to Ball et al, 2016 for a detailed description of this method (Ball et al., 2016). Briefly,  
377 cells were incubated (1 h, 37°C, 0% CO<sub>2</sub>) before replacement of culture medium with 175 µL of  
378 unbuffered Seahorse XF base medium supplemented with glucose (25 mM), L-glutamine (2 mM),  
379 sodium pyruvate (1 mM), pre-warmed to 37°C (pH 7.4). Following an equilibration period,  
380 measurements were taken to establish a baseline oxygen consumption rate (OCR) prior to the acute  
381 injection of each of the five test compounds (7.8-500 µM). Following compound injection a  
382 mitochondrial stress test consisting, of sequential injections of oligomycin (ATP synthase inhibitor; 1  
383 µM), carbonyl cyanide 4-(trifluoromethoxy) phenylhydrazone (FCCP) (uncoupler; 0.5 µM) and  
384 rotenone/antimycin A (complex I/III inhibitors respectively; 1 µM each), was performed.

385 *Respiratory complex assays*

386 Please refer to Salabei et al, 2014 for a detailed description of this method (Salabei et al., 2014).  
387 Briefly, culture medium was replaced with mitochondrial assay solution buffer (MAS: MgCl<sub>2</sub>; 5 mM,  
388 mannitol; 220 mM, sucrose; 70 mM, KH<sub>2</sub>PO<sub>4</sub>; 10 mM, HEPES; 2 mM, EGTA; 1 mM, BSA; 0.4% w/v)  
389 containing constituents to permeabilise cells and stimulate oxygen consumption via complex I (ADP;  
390 4.6 mM, malic acid; 30 mM, glutamic acid; 22 mM, BSA; 30 µM, PMP; 1 nM), complex II (ADP; 4.6  
391 mM, succinic acid; 20 mM, rotenone; 1 µM, BSA; 30 µM, PMP; 1 nM), complex III (ADP; 4.6 mM,  
392 duroquinol; 500 µM, rotenone; 1 µM, malonic acid; 40 µM, BSA; 0.2% w/v, PMP; 1 nM) or complex  
393 IV (ADP; 4.6 mM, ascorbic acid; 20 mM, TMPD (N,N,N',N'-tetramethyl-p-phenylenediamine); 0.5  
394 mM, antimycin A; 2 mM, BSA; 30 mM, PMP; 1 nM). Following a basal measurement (no equilibration  
395 period) of three cycles of mix (30 s), wait (30 s) and measure (2 min), flutamide or 2-  
396 hydroxyflutamide (or MAS buffer for determination of basal complex activity) was injected followed  
397 by a mitochondrial stress test as detailed previously, only each measurement cycle was 3 min rather  
398 than 6 min.

399 *Statistical analysis*

400 In total 10 distinct cybrid cell lines were generated, one from each recruited volunteer, specifically 5  
401 x distinct haplogroup H cell lines, and 5 x distinct haplogroup J cell lines. Additionally, 5 cybrid  
402 populations were generated for each cell line (volunteer). Each population was tested as an  
403 independent experiment (n =1), therefore giving a total of n=5 for each cybrid cell line/volunteer.  
404 Each independent experiment contained a minimum of 3 technical replicates.

405 Platelets were provided to the investigator blinded to haplogroup, to avoid bias; therefore, cybrid  
406 generation, experiments and subsequent data analyses were performed on cybrids for which the

407 haplogroup was unknown. Unblinding occurred at the stage at which datasets were combined to the  
408 to enable the subsequent statistical comparison of haplogroup H vs haplogroup J.

409 Parameters for comparison were predefined to discourage statistical bias during analyses. These  
410 were, for both the assessment of mitochondrial function and drug-induced mitochondrial  
411 dysfunction: basal, maximum and ATP-linked respiration, spare respiratory capacity, proton leak and  
412 complex I-IV activity. Normality was assessed using a Shapiro-Wilk test. All data were assessed as  
413 parametric and therefore statistical significance was determined by an unpaired t-test using  
414 GraphPad Prism Version 7.0. Significance was determined when p value <0.05. EC<sub>50</sub> data were  
415 determined by nonlinear regression analysis using GraphPad Prism 7.0 for the assessment of drug  
416 treatment on ATP level.

## 417 References

418 Alfirevic A, Gonzalez-Galarza F, Bell C et al (2012) In silico analysis of HLA associations with drug-  
419 induced liver injury: use of a HLA-genotyped DNA archive from healthy volunteers. *Genome Med*  
420 4:51. doi: 10.1186/gm350.

421 Amuthan, G., Biswas, G., Ananadatheerthavarada, H.K., Vijayasathy, C., Shephard, H.M., and  
422 Avadhani, N.G. (2002). Mitochondrial stress-induced calcium signaling, phenotypic changes and  
423 invasive behavior in human lung carcinoma A549 cells. *Oncogene* 21: 7839–7849. doi:  
424 10.1038/sj.onc.1205983.

425 Bale, S.S., Vernetti, L., Senutovitch, N., Jindal, R., Hegde, M., Gough, A., et al. (2014). In Vitro  
426 Platforms for Evaluating Liver Toxicity. *Exp. Biol. Med.* (Maywood). 239: 1180–1191. doi:  
427 10.1177/1535370214531872.

428 Ball, A.L., Bloch, K.M., Rainbow, L., Liu, X., Kenny, J., Lyon, J.J., et al. (2021). Assessment of the impact  
429 of mitochondrial genotype upon drug-induced mitochondrial dysfunction in platelets derived from  
430 healthy volunteers. *Arch. Toxicol.* 1–13. doi: 10.1007/s00204-021-02988-3

431 Ball, A.L., Kamalian, L., Alfirevic, A., Lyon, J.J., and Chadwick, A.E. (2016). Identification of the  
432 Additional Mitochondrial Liabilities of 2-Hydroxyflutamide When Compared With its Parent  
433 Compound, Flutamide in HepG2 Cells. *Toxicol Sci.* doi: 10.1093/toxsci/kfw126.

434 Benabou, R., and Waters, C. (2003). Hepatotoxic profile of catechol-O-methyltransferase inhibitors  
435 in Parkinson's disease. *Expert Opin. Drug Saf.* 2: 263–267. doi: 10.1517/14740338.2.3.263.

436 Bernal, W., and Wendon, J. (2013). Acute liver failure. *N. Engl. J. Med.* 369: 2525–2534. doi:  
437 10.1056/NEJMra1208937.

438 Coe, K.J., Jia, Y., Ho, H.K., Rademacher, P., Bammler, T.K., Beyer, R.P., et al. (2007). Comparison of  
439 the cytotoxicity of the nitroaromatic drug flutamide to its cyano analogue in the hepatocyte cell line  
440 TAMH: evidence for complex I inhibition and mitochondrial dysfunction using toxicogenomic  
441 screening. *Chem Res Toxicol* 20: 1277–1290. doi: 10.1021/tx7001349.

442 Dykens, J.A., and Will, Y. (2007). The significance of mitochondrial toxicity testing in drug  
443 development. *Drug Discov. Today* 12: 777–785.



- 444 Eupedia (2016). European MtDNA Haplogroups Frequency.
- 445 Fermi, B., Coyne, K.P., and Coyne, S.T. (2018). Challenges in designing and executing clinical trials  
446 in a dish studies. *J. Pharmacol. Toxicol. Methods* 94: 73–82. doi: 10.1016/j.vascn.2018.09.002.
- 447 Fontana, R.J. (2014). Pathogenesis of Idiosyncratic Drug-Induced Liver Injury and Clinical  
448 Perspectives. *Gastroenterology* 146: 914–928. doi: 10.1053/j.gastro.2013.12.032.
- 449 Ghelli, A., Porcelli, A.M., Zanna, C., Vidoni, S., Mattioli, S., Barbieri, A., et al. (2009). The background  
450 of mitochondrial DNA haplogroup J increases the sensitivity of Leber’s hereditary optic neuropathy  
451 cells to 2,5-hexanedione toxicity. *PLoS One* 4: e7922. doi: 10.1371/journal.pone.0007922.
- 452 Jones SW, Ball AL, Chadwick AE, Alfirevic A. The Role of Mitochondrial DNA Variation in Drug  
453 Response: A Systematic Review. *Front Genet.* 2021a Aug 17;12:698825. doi:  
454 10.3389/fgene.2021.698825.
- 455 Jones, S.W., Penman, S.L., French, N.S., Park, B.K., and Chadwick, A.E. (2021b). Investigating  
456 dihydroorotate dehydrogenase inhibitor mediated mitochondrial dysfunction in hepatic in vitro  
457 models. *Toxicol. Vitro.* 72: 105096. doi: 10.1016/j.tiv.2021.105096.
- 458 King, M.P., and Attardi, G. (1989). Human cells lacking mtDNA: repopulation with exogenous  
459 mitochondria by complementation. *Science* (80-. ). 246: 500–503. doi: 10.1126/science.2814477.
- 460 Lees, A.J. (2008). Evidence-based efficacy comparison of tolcapone and entacapone as adjunctive  
461 therapy in Parkinson’s disease. *CNS Neurosci. Ther.* 14: 83–93. doi: 10.1111/j.1527  
462 3458.2007.00035.
- 463 Leise, M.D., Poterucha, J.J., and Talwalkar, J.A. (2014). Drug-induced liver injury. *Mayo Clin Proc* 89:  
464 95–106. doi: 10.1016/j.mayocp.2013.09.016.
- 465 Longo, D.M., Yang, Y., Watkins, P.B., Howell, B.A., and Siler, S.Q. (2016). Elucidating Differences in  
466 the Hepatotoxic Potential of Tolcapone and Entacapone With DILISym((R)), a Mechanistic Model of  
467 Drug-Induced Liver Injury. *CPT Pharmacometrics Syst. Pharmacol.* 5: 31–39. doi:  
468 10.1002/psp4.12053.
- 469 Luo, Y., Bond, J.D., and Ingram, V.M. (1997). Compromised mitochondrial function leads to increased  
470 cytosolic calcium and to activation of MAP kinases. *Proc. Natl. Acad. Sci.* 94: 9705–9710. doi:  
471 10.1073/pnas.94.18.9705.
- 472 Olanow, C.W. (2000). Tolcapone and hepatotoxic effects. Tasmar Advisory Panel. *Arch. Neurol.* 57:  
473 263–267. doi: 10.1001/archneur.57.2.263.
- 474 Olanow, C.W., and Watkins, P.B. (2007). Tolcapone: an efficacy and safety review. *Clin.  
475 Neuropharmacol.* 30: 287–294. doi: 10.1097/wnf.0b013e318038d2b6.
- 476 Oven, M. Van, and Kayser, M. (2009). Updated comprehensive phylogenetic tree of global human  
477 mitochondrial DNA variation. *Hum Mutat* 30(2):E386-94. doi: 10.1002/humu.20921.
- 478 Penman, S.L., Carter, A.S., and Chadwick, A.E. (2020). Investigating the importance of individual  
479 mitochondrial genotype in susceptibility to drug-induced toxicity. *Biochem. Soc. Trans.* 48: 787–797.  
480 doi: 10.1042/BST20190233.
- 481 Rivest, J., Barclay, C.L., and Suchowersky, O. (1999). COMT inhibitors in Parkinson’s disease. *Can. J.  
482 Neurol. Sci.* 26 Suppl 2: S34-8. doi: 10.1017/s031716710000007x.

483 Salabei, J.K., Gibb, A.A., and Hill, B.G. (2014). Comprehensive measurement of respiratory activity in  
484 permeabilized cells using extracellular flux analysis. *Nat. Protoc* 9: 421–438. doi:  
485 10.1038/nprot.2014.018.

486 Shet, M.S., McPhaul, M., Fisher, C.W., Stallings, N.R., and Estabrook, R.W. (1997). Metabolism of the  
487 antiandrogenic drug (Flutamide) by human CYP1A2. *Drug Metab. Dispos* 25: 1298–1303.

488 Sison-Young, R.L., Mitsa, D., Jenkins, R.E., Mottram, D., Alexandre, E., Richert, L., et al. (2015).  
489 Comparative Proteomic Characterization of 4 Human Liver-Derived Single Cell Culture Models  
490 Reveals Significant Variation in the Capacity for Drug Disposition, Bioactivation, and Detoxication.  
491 *Toxicol Sci* 147: 412–424. doi: 10.1093/toxsci/kfv136.

492 Srinivasan, S., Guha, M., Dong, D.W., Whelan, K.A., Ruthel, G., Uchikado, Y., et al. (2015). Disruption  
493 of cytochrome c oxidase function induces the Warburg effect and metabolic reprogramming.  
494 *Oncogene*. doi: 10.1038/onc.2015.227.

495 Tujjos, S.R., and Lee, W.M. (2018). Acute liver failure induced by idiosyncratic reaction to drugs:  
496 challenges in diagnosis and therapy. *Liver Int.* 38: 6–14. doi: 10.1111/liv.13535.

497 Watkins, P. (2000). COMT inhibitors and liver toxicity. *Neurology* 55: S51-2; discussion S53-6.

498 Wilkins, H.M., Carl, S.M., and Swerdlow, R.H. (2014). Cytoplasmic hybrid (cybrid) cell lines as a  
499 practical model for mitochondriopathies. *Redox Biol.* 2: 619–631. doi: 10.1016/j.redox.2014.03.006.

## 500 Article and Author Information

501 **Funding statement:** This work was supported by the Centre for Drug Safety Science supported by  
502 the Medical Research Council, United Kingdom (Grant Number G0700654); and GlaxoSmithKline as  
503 part of an MRC-CASE studentship (grant number MR/L006758/1).

504 **Acknowledgements:** The authors would like to thank the Royal Liverpool Research Facility, in  
505 particular, Lisa Gaskell, for the recruitment of volunteers and sample collection, and Prof. Dr. Peter  
506 Seibel and colleagues for their assistance in the generation of rho zero cells.

507 **Authors' contributions:** Author A.L.B generated the cybrid models, contributed to study design,  
508 completed laboratory work and data analysis, and wrote the manuscript. Author C.E.J contributed  
509 towards the generation of cybrid models and study design, and provided critical feedback. Author J.J  
510 contributed towards project conceptualisation. Author A.A contributed to funding acquisition,  
511 project conceptualisation and securement of resources including collaboration with the Royal  
512 Liverpool Research Facility. Author A.E.C acquired funding, conceptualised the project, directed data  
513 analysis and provided critical feedback. All authors have approved the final manuscript.

514 **Competing interests:** J.J.L is affiliated with GSK GlaxoSmithKline. The other authors declare no  
515 competing interests that pertain to this work.

516 **Ethics approval statement:** All procedures performed in studies involving human participants were  
517 in accordance with the ethical standards of the North West of England Research Ethics Committee



518 (Cell Archive of HLA Typed Healthy Volunteers (HLA), CRN ID 7787, IRAS ID: 15623) with the 1964  
 519 Helsinki declaration and its later amendments or comparable ethical standards.

520 **Data availability:** Source data are provided as files linked to the appropriate table/figures.

521 **Supplementary Information**

522 *Mitochondrial DNA (MtDNA) variation of 10 healthy volunteers whose platelets were used to generate*  
 523 *cybrids*

Donor	Haplogroup	Subhaplogroup	SNPs characteristic of assigned haplogroup	Additional SNPs
1	H	H1c3	257G 263G 477C 750G 1438G 3010A 4769G 8473C 8860G 15326G	195C 12966T 16519C
2	H	H1bb	152C 263G 750G 1438G 3010A 4769G 8860G 11864C 15326G	16519C
3	H	H1a1	73G 263G 750G 1438G 3010A 4769G 6365C 8860G 15326G 16162G	152C 3483A 16360T 16519C
4	H	H1c	263G 477C 750G 1438G 3010A 4769G 8860G 15326G	10646A 16519C
5	H	H2a1e1a1	263G 575T 750G 751G 951A 8860G 15326G 16124C 16148T 16166G 16354T	
6	J	J2b1g	73G 150T 152C 263G 489C 750G 1438G 4769G 5633T 7028T 8860G 9872G 10172A 10398G 11251G 11719A 12612G 13708A 14766T 15257A 15326G 15452A 15812A 16069T 16126C 16193T	2789T 13821T
7	J	J1c+16261	73G 185A 228A 263G 295T 462T 489C 750G 1438G 3010A 4216C 4769G 7028T 8860G 10398G 11251G 11719A 12612G 13708A 14766T 14798C 15326G 15452A 16069T 16126C 16261T	4113A 6554T 10915C 16316G
8	J	J1c1c	185A 228A 462T 482C 489C 750G 1438G 3010A 3394C 4216C 4769G 7028T 8860G 10398G 11251G 11719A 13708A 14766T 14798C 15326G 15452A 16069T 16126C 16145A	188G 13943T 14552G
9	J	J1c2h	185A 188G 222T 228A 263G 295T 462T 489C 750G 1438G 3010A 4216C 4769G 7028T 8860G 10398G 11251G 11719A 12612G 13708A 14766T 14798C 15326G 15452A 16069T 16126C	16189C 16519C 16527T
10	J	J1c1e	185A 228A 263G 295T 462T 482C 489C 750G 1438G 3010A 3394C 4216C 4769G 7028T 8860G 10398G 10454C 11251G 11719A 12612G 13708A 14766T 14798C 15326G 15452A 16069T 16126C 16368C	13889A

524 Additional SNPs refers to SNPs that were present in the sample but were not characteristic of the assigned haplogroup.  
 525 Abbreviations: SNP, single nucleotide polymorphism.

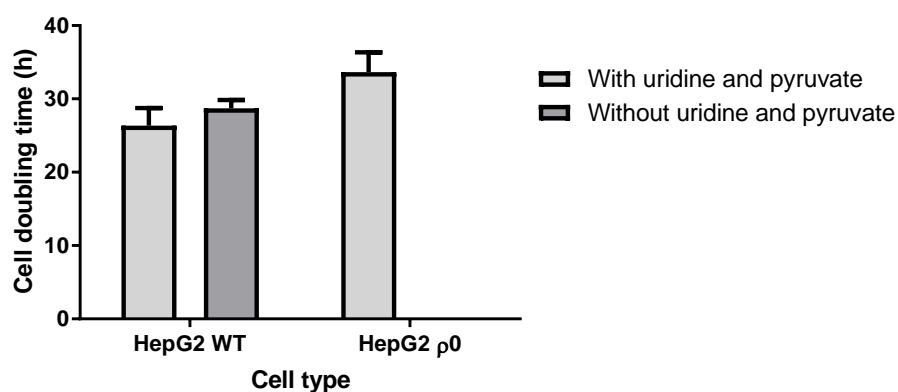
526

527 *Characterisation of HepG2 rho zero cells and HepG2 transmitochondrial cybrids*

528

529 *S1: Cell doubling time*

530 The dependence of HepG2  $\rho 0$  cells on pyruvate and uridine meant that culture media devoid of  
 531 these constituents was able to select for the successful depletion of mtDNA and the resultant non-  
 532 functional electron transport chain in EtBr-treated cells. Concordantly, HepG2 WT cells had a similar  
 533 doubling time in media with or without these additives, averaging 26.2 hours. In contrast, HepG2  $\rho 0$   
 534 cells exhibited no growth without uridine and pyruvate and an average doubling time of 27.6 hours



535 when in media containing these two constituents.

536 **Cell doubling time of HepG2 wild-type (WT) and HepG2 rho zero ( $\rho 0$ ) cells.** The two cell types were cultured in media with  
 537 or without uridine and pyruvate and growth rate calculated. Data are presented as mean+SEM of n=3 experiments. Source  
 538 data: figs s1 – source data file.xlsx

539 *S2: Mitochondrial DNA content*

540 The Ct value of both mtDNA primers increased dramatically in  $\rho 0$  compared to WT cells whilst  
 541 nuclear DNA Ct values remained consistent across all three cell lines. Similarly, both HepG2 WT and  
 542 cybrid cells had thousands of mtDNA copies/cell in contrast to the  $\rho 0$  cells which had less than one  
 543 copy/cell

544 **Assessment of mtDNA content in HepG2 wild-type (WT), HepG2 rho zero ( $\rho 0$ ) and HepG2 cybrids.**

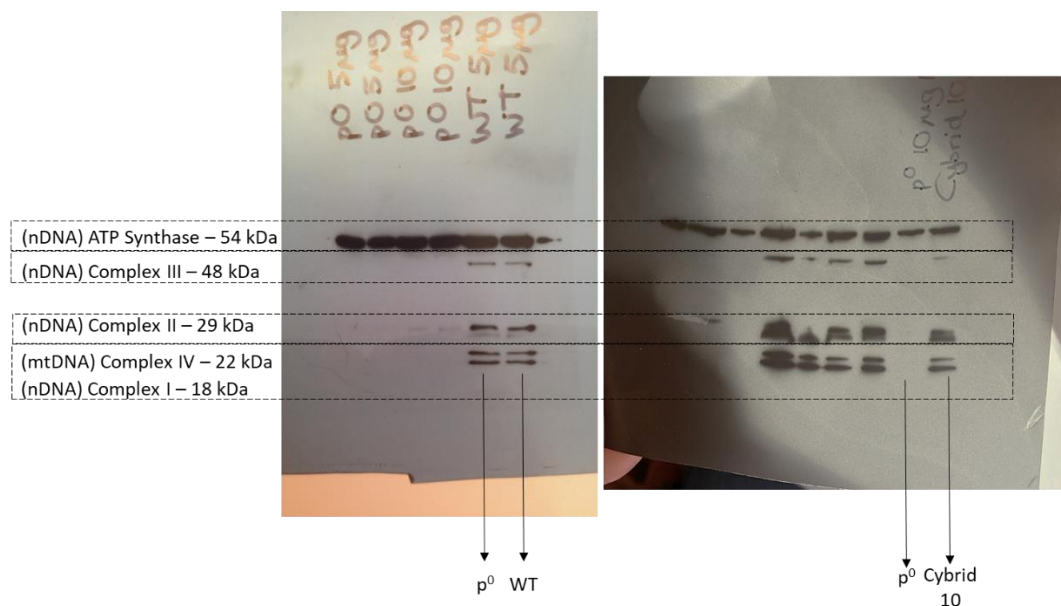
Sample	Primer C <sub>t</sub> value				mtDNA copies/cell			
	TERT	RNase P	ND-1	Custom	TERT/ ND-1	TERT/ custom	RNase P/ ND-1	RNase P/ custom
HepG2 WT	30.6 (1.00)	31.3 (1.11)	18.5 (0.120)	18.9 (0.140)	9280	6985	14563	10960
HepG2 $\rho 0$	27.7 (0.0600)	27.2 (0.0700)	34.7 (0.740)	32.0 (0.180)	0.00400	0.0240	0.00300	0.0170
HepG2	29.8 (1.10)	30.4 (0.550)	18.9 (0.730)	19.0 (0.0900)	3875	3590	5673	5256

cybrid								
--------	--	--	--	--	--	--	--	--

545 Abbreviations:  $C_t$ , cycle threshold; ND-1, NADH dehydrogenase-1; RNase, ribonuclease P RNA component H1; TERT,  
546 telomerase reverse transcriptase; WT, wild-type;  $\rho_0$ , rho zero.  $C_t$  values are displayed as mean (SEM).

547 S3: Detection of mitochondrial/nuclear DNA-encoded mitochondrial proteins

548 Western blot analysis showed expression of all nuclear DNA and mtDNA-encoded subunits of the  
549 electron transport chain which were probed for in HepG2 WT and cybrid cells. However,  $\rho_0$  cells did  
550 not express the mtDNA-encoded subunit of complex IV. Notably, despite all the other subunits being  
551 encoded in the nuclear DNA, it was only the alpha subunit of ATP synthase that was retained in the  
552  $\rho_0$  cells.



553 **Representative western blots of HepG2 wild-type (WT), rho zero and cybrid cell lysates.** 10  $\mu$ g of lysate protein was  
554 resolved by SDS-PAGE and probed for subunits of complexes I (NDUFB8), II (Iron-sulphur protein (IP) 30 kDa), III (Core 2), IV  
555 (II), V (alpha). Abbreviations: mtDNA, mitochondrial DNA; nDNA, nuclear DNA. Source data: figs s3 and s4 source data  
556 file.xlsx and figs s3 –raw data.pptx  
557

558

559 S4: Detection of electron transport chain function

560 HepG2 WT and cybrid cells exhibited a classic response to the series of mitochondrial inhibitors used  
561 to perform the mitochondrial stress test whereas the  $\rho_0$  cells did not respond to these inhibitors and  
562 had very low basal OCR, all of which was due to non-mitochondrial respiration. The PPRgly /OCR  
563 ratio was also higher in WT and  $\rho_0$  cells compared with cybrid cells.

564 **Differences in parameters of mitochondrial function in HepG2 wild-type (WT), rho zero ( $\rho_0$ ) and cybrid cells.**

HepG2 cell type	Basal OCR (pmol/min/ $\mu$ g protein)	PPR <sub>gly</sub> /OCR	% Non-mitochondrial respiration
WT	6.52 (0.350)	0.354 (0.0900)	28.4 (0.310)

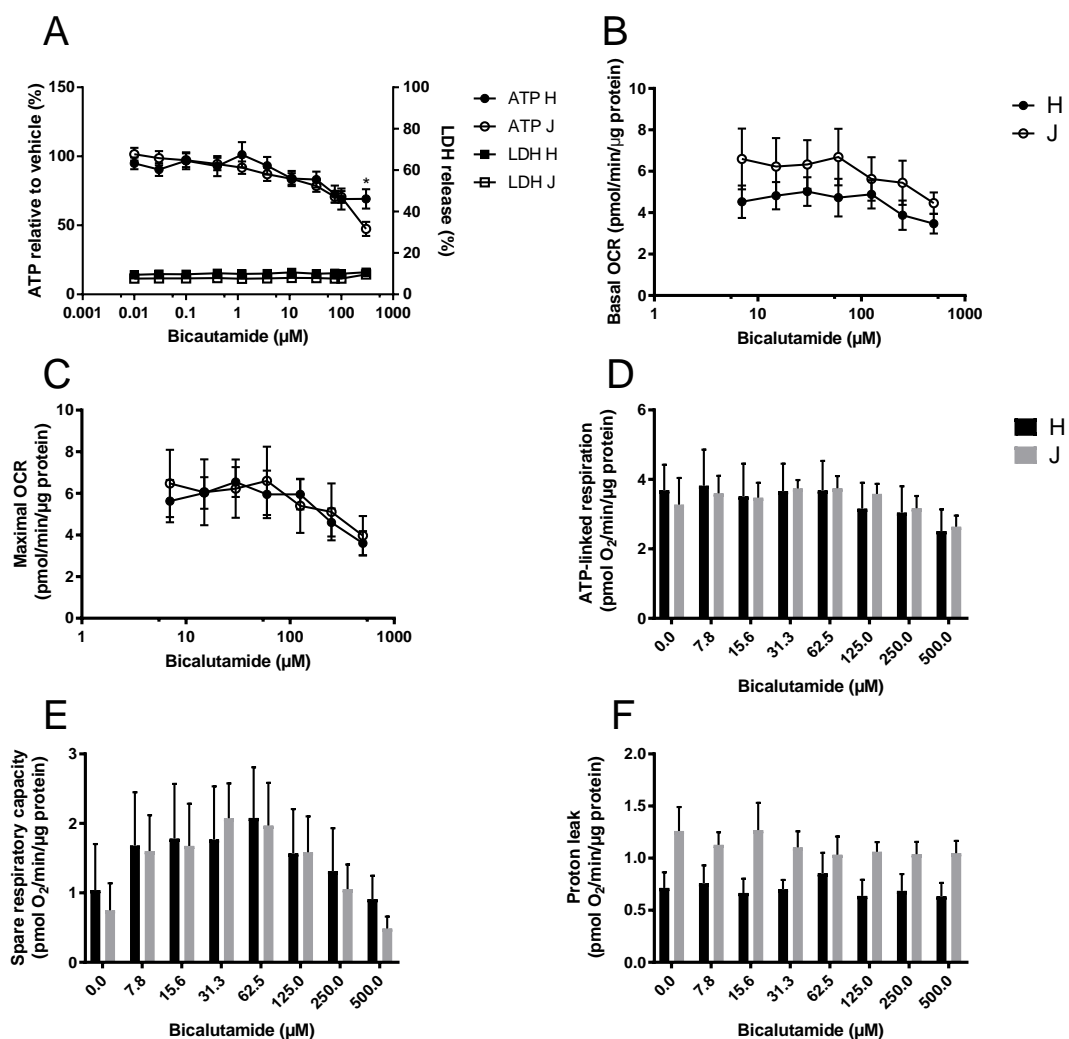
Rho zero	0.450 (0.100)	55.5 (0.930)	102 (4.33)
Cybrid	6.53 (0.400)	0.466 (0.660)	24.3 (0.510)

565 Abbreviations: OCR, oxygen consumption rate; PPR<sub>gly</sub>, proton production rate attributed to glycolysis; WT, wild-type.

566 Values are displayed as mean (SEM). Source data: figs s3 and s4 source data file.xlsx

567 *S5: The effect of bicalutamide upon haplogroup H and J trans-mitochondrial cybrids*

568 Bicalutamide-treated cybrids of each haplogroup exhibited a similar decline in ATP content  
 569 until the highest concentration used (300  $\mu$ M), when haplogroup J cybrids had significantly  
 570 less ATP (Figure A). As with flutamide and 2-hydroxyflutamide treatment, the decline in ATP  
 571 was in the absence of significant LDH release. No significant differences were evident  
 572 between the two cybrids groups in parameters of mitochondrial function using XF analysis,  
 573 however as was the case with flutamide and 2-hydroxyflutamide, haplogroup J exhibited  
 574 higher proton leak in both control and treated cybrids (Figure B-F).



575 **The effect of bicalutamide upon ATP levels and mitochondrial respiratory function in haplogroup H and J HepG2 cybrids.**

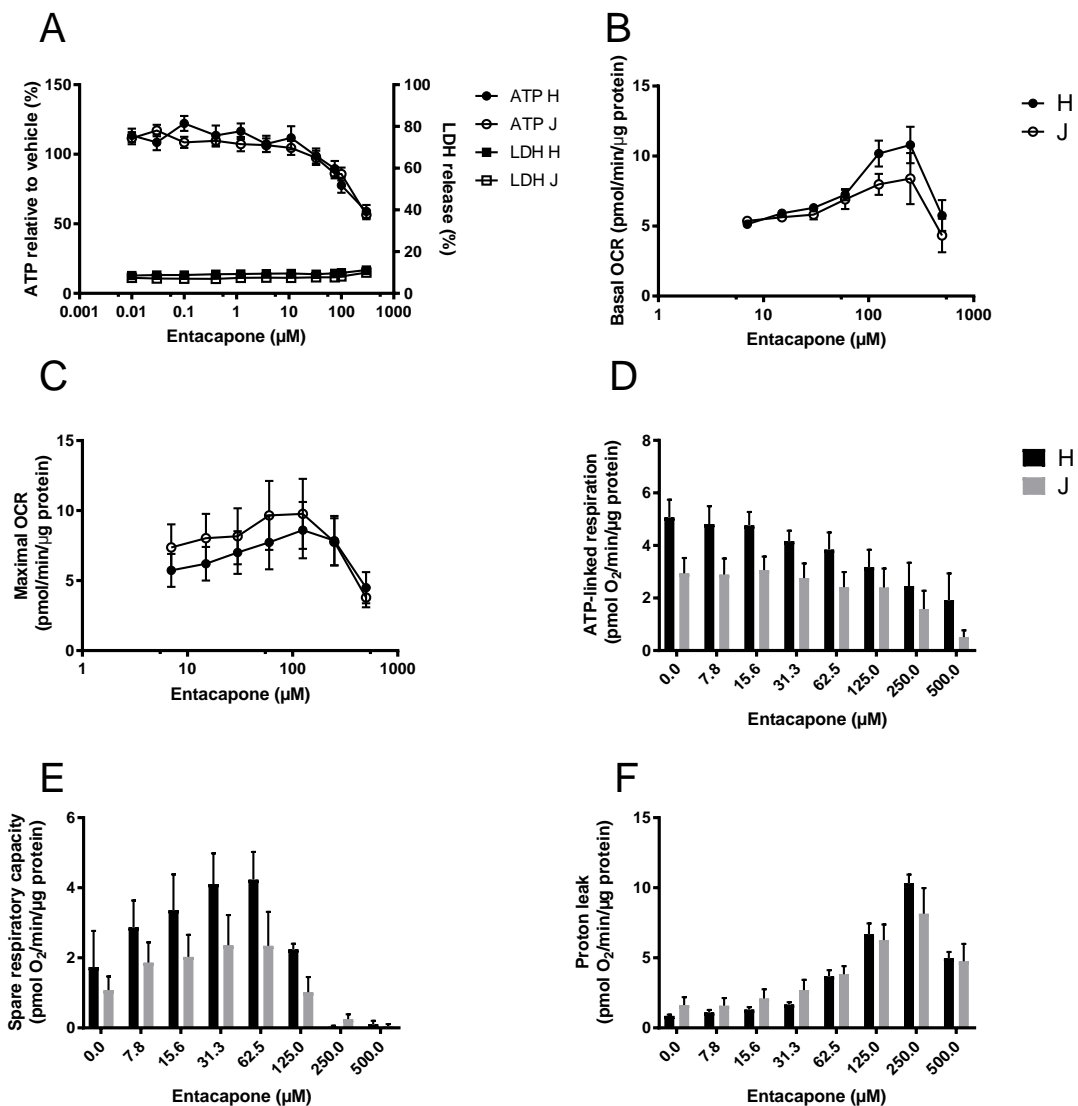
576 **A:** Cybrids were treated (2 h) up to 300  $\mu$ M bicalutamide in galactose medium. ATP values are expressed as a percentage of

577 those of the vehicle control. Lactate dehydrogenase (LDH) release is expressed as extracellular LDH as a % of total LDH. **B-F:**  
 578 XF analysis-detected changes in basal and maximal respiration, ATP-linked respiration, spare respiratory capacity and  
 579 proton leak following acute treatment with bicalutamide (up to 500  $\mu\text{M}$ ). Statistical significance between haplogroup H and  
 580 J cybrids: \*  $p < 0.05$ . Data are presented as mean  $\pm$  SEM of  $n = 5$  experiments. Source data: figs s5 – source data file.xlsx

581

582 *S6: The effect of entacapone upon haplogroup H and J transmitochondrial cybrids*

583 Entacapone induced a weaker decline in ATP levels compared to tolcapone (Figure A). There  
 584 was no significant difference in ATP levels between the two haplogroups and also no  
 585 significant difference in parameters of mitochondrial function, though haplogroup H cybrids  
 586 had consistently higher ATP-linked respiration and spare respiratory capacity which tended  
 587 towards significance (Figure D, E).



588

589 The effect of entacapone upon ATP levels and mitochondrial respiratory function in haplogroup H and J HepG2  
 590 transmitochondrial cybrids. **A:** Cybrids were treated (2 h) with serial concentrations up to 300  $\mu\text{M}$  entacapone in galactose

591 medium. ATP values are expressed as a percentage of those of the vehicle control. Lactate dehydrogenase (LDH) release is  
592 expressed as extracellular LDH as a % of total LDH. **B-F:** Changes in basal respiration, maximal respiration, ATP-linked  
593 respiration, spare respiratory capacity and proton leak following acute treatment with entacapone (up to 500  $\mu$ M). Data  
594 are presented as mean  $\pm$  SEM of n = 5 experiments. Source data: figs s6 – source data file.xlsx

## 595 Appendix: Supplementary Methods

596

### 597 *Methodology*

#### 598 Cell doubling time

599 HepG2 wild-type (WT) cells and HepG2 rho zero ( $\rho$ 0) cells were seeded at 30 000 cells/well in a  
600 24-well plate in either  $\rho$ 0 cell media (contains pyruvate and uridine) or selection media (devoid of  
601 pyruvate and uridine). On days 1, 3, 5 and 7 of culture, cells were collected by trypsinisation and  
602 counted, following which growth rate was calculated. Rho zero cells are auxotrophic for pyruvate  
603 and uridine, but WT cells are not, therefore the absence of cell growth in selection media indicated  
604 complete loss of mtDNA.

#### 605 DNA extraction and real-time PCR

606 DNA extraction from HepG2 WT, HepG2  $\rho$ 0 and HepG2 cybrid cells was performed using a DNA mini  
607 kit (Qiagen, Manchester, UK) according to the manufacturer's instructions. Sample DNA  
608 concentrations and quality were then quantified using a Quant-iT<sup>TM</sup> PicoGreen<sup>TM</sup> dsDNA Assay Kit  
609 and nanodrop spectrophotometry respectively (Fischer Scientific, Loughborough, UK).

610 Real-time PCR was carried out using two primers for regions of mtDNA; a custom sequence and ND-  
611 1 (complex I subunit) and two primers for regions of nuclear DNA; telomerase reverse transcriptase  
612 (TERT) and RNase P (Applied Biosystems, California, USA) (Malik et al., 2011).

613

**Real-time PCR primers used to amplify regions of mitochondrial and nuclear DNA.**

Gene	Dye/probe	Additional information
RNase P (nDNA)	VIC <sup>®</sup> dye-labelled TAMRA <sup>TM</sup> probe	Location: chromosome 14, cytoband 14q11.2
TERT (nDNA)	VIC <sup>®</sup> dye-labelled TAMRA <sup>TM</sup> probe	Location: chromosome 5, cytoband 5p15.33
Custom sequence (mtDNA)	FAM <sup>®</sup> dye-labelled MGB probe	Oligonucleotide sequences: <b>hmito F5</b> CTTCTGGCCACAGCACTTAAAC <b>hmito R5</b> GCTGGTGTAGGGTTCTTTGTTTT
ND-1 (mtDNA)	FAM <sup>®</sup> dye-labelled MGB probe	Location: mtDNA 3307-4262

614 Abbreviations: FAM, carboxyfluorescein; MGB, minor groove binder; ND-1, NADH dehydrogenase-1; mtDNA, mitochondrial  
615 DNA; TAMRA, 6-carboxytetramethyl-rhodamine; TERT, telomerase reverse transcriptase; VIC, 2'-chloro-7'-phenyl-1,4-  
616 dichloro-6-carboxy-fluorescein.

617 During sample preparation, 2X Taqman<sup>®</sup> genotyping master mix (5 µL), a nuclear DNA primer (0.5  
618 µL), mtDNA primer (0.5 µL), dH<sub>2</sub>O (2 µL) and 10 ng DNA (2 µL) from each sample were combined to  
619 give a final sample concentration of 1 ng/µL in each well. Real-time PCR was then carried out using  
620 the viiA7 RT-PCR system (Life Technologies, UK). MtDNA copies per cell were calculated on the basis  
621 that each nuclear DNA primer was present in diploid copies per cell and used the following formula,  
622 where  $x_1$ = nuclear DNA primer cycle threshold ( $C_t$ ) value,  $x_2$ =mtDNA primer  $C_t$  value: mtDNA copies  
623 per cell =  $2(2^{x_1 - x_2})$  (Schäfer, 2016).

#### 624 Detection of mitochondrial/nuclear DNA-encoded mitochondrial proteins

625 HepG2 p0, HepG2 WT or HepG2 cybrid cells were lysed using sonication and 10 µg of lysate protein  
626 was resolved by sodium dodecyl sulphate-polyacrylamide *gel* electrophoresis (SDS-PAGE) using 4-  
627 12% Bis-Tris gel (Invitrogen, UK) in MOPS buffer (MOPS; tris-base; 1.21% w/v, sodium dodecyl  
628 sulphate; 0.20% w/v, EDTA; 0.06% w/v in distilled water (dH<sub>2</sub>O)).

629 This gel was then transferred to a nitrocellulose membrane (GE Healthcare, Buckinghamshire, UK) in  
630 transfer buffer (tris-base; 0.30% w/v, glycine; 1.5% w/v, methanol; 20% v/v in dH<sub>2</sub>O) and blocked  
631 using 10% non-fat dried milk in Tris Buffered Saline-Tween (TBS-T: TBS; 0.50% v/v, tween; 0.10% v/v  
632 in dH<sub>2</sub>O).

633 Blocking solution was removed using TBS-T and the membrane probed for CI-20, CII-30, CIII-core2,  
634 CIV-I and CV-alpha subunits of complexes I-V of the electron transport chain using MitoProfile<sup>®</sup> Total  
635 OXPHOS Human WB Antibody Cocktail (Abcam, Cambridgeshire, UK) (0.20% v/v in 10% non-fat dried  
636 milk in TBS-T). This was followed by anti-mouse secondary antibody (0.01% v/v in 10% non-fat dried  
637 milk in TBS-T) before visualisation using an ECL<sup>™</sup> system (GE Healthcare, Buckinghamshire, UK).

#### 638 Detection of electron transport chain function

639 Mitochondrial stress tests were performed on untreated HepG2 WT, p0 and HepG2 cybrid cells using  
640 extracellular flux analysis as described in the main text.

641 Extracellular flux analysis produced two raw outputs, oxygen consumption rate and extracellular  
642 acidification rate (ECAR). ECAR can be indicative of the glycolytic rate of the cell, however it also  
643 takes into account changes in ECAR due to oxidative phosphorylation. Therefore the measure of  
644  $PPR_{gly}$ , glycolytic production rate was used to quantify glycolysis, this was calculated by subtracting  
645 respiratory acidification contributions from the total proton production rate.

$$PPR_{gly} = PPR_{tot} - PPR_{resp}$$

646 *Where*

$$PPR_{tot} = \frac{ECAR}{BP} \text{ and } PPR_{resp} = \left( \frac{10^{pH-6.093}}{1 + 10^{pH-6.093}} \right) \left( \frac{\max H^+}{O_2} \right) (OCR_{tot} - OCR_{rot})$$

647 **Equations for the calculation of  $PPR_{gly}$  from mitochondrial stress tests.** Abbreviations:  $PPR_{gly}$ , proton  
648 production rate attributed to glycolysis;  $PPR_{resp}$ , proton production rate attributed to respiration;  $PPR_{tot}$ , total  
649 proton production rate; ECAR, extracellular acidification rate; BP, buffering power;  $\max H^+/O_2$ , derived  
650 acidification for metabolic transformation of glucose oxidation;  $OCR_{tot}$ , total oxygen consumption rate;  $OCR_{rot}$ ,  
651 oxygen consumption rate following rotenone injection (Kelly, 2018).

## 652 *Appendix References*

653 Kelly, R. (2018). Biochemical Thermodynamic Modelling of Cellular Bioenergetics: A Quantitative  
654 Systems Pharmacology Approach. Liverpool John Moores University.

655 Malik, A.N., Shahni, R., Rodriguez-de-Ledesma, A., Laftah, A., and Cunningham, P. (2011).  
656 Mitochondrial DNA as a non-invasive biomarker: Accurate quantification using real time quantitative  
657 PCR without co-amplification of pseudogenes and dilution bias. Biochem. Biophys. Res. Commun.  
658 412: 1–7.

659 Schäfer, I. University of Leipzig (2016). Personal Communication.

660

661